Journal of Hydrology: Regional Studies 44 (2022) 101270

Contents lists available at ScienceDirect

Journal of Hydrology: Regional Studies

journal homepage: www.elsevier.com/locate/ejrh

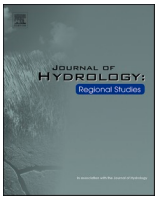

A new drought monitoring approach using three-dimensional drought properties based on a dynamic drought detection technique algorithm

Jiyoung Yoo [a], Jiyoung Kim [b], Hyun-Han Kwon [c], Tae-Woong Kim [d,*]

[a] Research Institute of Engineering and Technology, Hanyang University, Ansan 15588, South Korea
[b] Department of Smart City Engineering, Hanyang University, Seoul 04763, South Korea
[c] Department of Civil and Environmental Engineering, Sejong University, Seoul 05006, South Korea
[d] Department of Civil and Environmental Engineering, Hanyang University, Ansan 15588, South Korea

ARTICLE INFO

Keywords:
3D-drought event
Central Asia
Dynamic drought map
Drought monitoring
Drought trajectory
Spatiotemporal analysis
SPEI-HR

ABSTRACT

Study region: Central Asia.
Study focus: In Central Asia, there is a lack of drought information to help understand the spatiotemporal variability and evolutionary characteristics of droughts. In this study, drought analysis data (i.e., high-resolution Standardized Precipitation Evapotranspiration Index (SPEI) dataset) was utilized in consideration of the meteorological and topographical characteristics of Central Asia and a dynamic drought detection technique (DDDT) algorithm was proposed for extracting three-dimensional(3D) drought events. As a result, it was possible to analyze the spatiotemporal distribution patterns and characteristics of droughts, which are intertwined with spatiotemporal dimensions. The drought events in Central Asia during the period of 1981–2018 were identified and their spatiotemporal distribution patterns and variabilities were characterized using various drought characteristic indicators (drought duration, severity, affected area, intensity, location (latitude and longitude), and the distance and direction of the drought trajectory). Finally, a new approach to monitoring conditional drought in Central Asia was proposed based on a dynamic drought map that includes all 3D-drought properties.
New hydrological insights for the region: Our major findings include (i) high-resolution data sets are suitable to interpret the development process and evolutionary characteristics of drought in consideration of the climatic and various topographical characteristics of Central Asia, (ii) most droughts of large and small scale in Central Asia can be quantified by identifying drought events in a three-dimensional concept using a DDDT algorithm, (iii) the direction of the drought trajectory that occurred in the study area during the period of 1981–2018 was often lateral, i.e., east and west, and (iv) in Central Asia at the beginning of 2008, severe drought continued in 2008, although the number of new monthly droughts tended to decrease. As a result of identifying the cause using the dynamic drought map, the number of new droughts that occurred every month in the second half of 2007 tended to increase, which led to the long-term drought in 2008.

* Corresponding author.
E-mail addresses: 7924pooh@hanyang.ac.kr (J. Yoo), jiy117@hanyang.ac.kr (J. Kim), hkwon@sejong.ac.kr (H.-H. Kwon), twkim72@hanyang.ac.kr (T.-W. Kim).

https://doi.org/10.1016/j.ejrh.2022.101270
Received 1 June 2022; Received in revised form 22 October 2022; Accepted 18 November 2022
Available online 22 November 2022
2214-5818/© 2022 The Author(s). Published by Elsevier B.V. This is an open access article under the CC BY-NC-ND license (http://creativecommons.org/licenses/by-nc-nd/4.0/).

1. Introduction

Drought is a natural recurring phenomenon that occurs everywhere at various points in time. Drought is a complex topic which has impacts on different ecosystems, depending on the intensity and duration, and socio-economic impacts that often magnify the problems of the most vulnerable members of society. Since 1974, drought has claimed more than one million lives and caused $60 billion in damage throughout the world (United Nations (UN), 2008). A thorough understanding of drought is essential to mitigate the current drought risk and prepare for climate change.

Central Asia is characterized by complex geographic landscapes, shortages of water resources, agriculture-led economies, and growing populations. In addition, Central Asia has a predominantly arid/semiarid climate that is particularly sensitive to changes of atmospheric circulation. As such, the region, even in slightly drier years, has endured significant agricultural production losses, destruction of local economies, and threats to social stability (Broka et al., 2016). Clearly, developing drought prevention and preparedness strategies requires a better understanding of the spatiotemporal variability of drought and its evolutionary nature (Liu et al., 2018; Wen et al., 2018).

Since drought is a regional phenomenon that occurs over a long period of time, it is important to understand the spatial characteristics of drought. Previous studies on droughts, mainly before 2005, focused on the analysis of spatial patterns using data available in the target area. For example, statistical methods, such as correlation analysis and empirical orthogonal functions, can be used to estimate the regional characteristics of droughts (Oladipo, 1986; Cook et al., 1999; Hisdal and Tallaksen, 2003; Diaz et al., 2020; Andreadis et al., 2005) proposed a method for estimating the drought severity-area-duration, which is used to track drought duration according to the spatial changes of drought severity using a grid-based hydrological model. However, focusing on spatial characteristics obscures much of the temporal evolution of droughts. Therefore, it is essential to analyze the spatiotemporal structures of droughts to understand the role of external and internal forcing in drought progression.

Subsequent studies have applied a global severity-area-duration curve analysis (Sheffield et al., 2009; Zhan et al., 2016). Drought cluster characteristics (e.g., distribution of centroids, the direction of displacement over time, and changes in a cluster area, intensity, and severity) have been studied at national (Vicente-Serrano, 2006; Vidal et al., 2010; Xu et al., 2015; Zhai et al., 2016) and continental (Lloyd-Hughes, 2012) scales. However, previous studies were limited to simple assessments of drought regions using time series of drought severity or report aggregation (Vicente-Serrano, 2006; Vidal et al., 2010; Gocic and Trajkovic, 2014; Wang et al., 2015).

Many researchers analyzed drought events with relatively long durations and large impact areas in spatiotemporal drought interpretations. In other words, minor drought events have generally been filtered out so as not to affect the identification of major drought events. For example, Diaz et al. (2020) showed that after first filtering the largest cluster (the cluster with the largest area) at each time step, the 3D drought onset and end time, duration, affected area, and spatiotemporal evolution were tracked and analyzed. However, such the 3D clustering algorithm has the problem of easily overlooking weak drought events.

In this study, we propose a practical method for monitoring droughts in space and time from a three-dimensional(3D) perspective and identifying all drought events in the Central Asia region during the period of 1981–2018 using high-resolution drought data. Various drought characterization factors (i.e., starting and ending time of drought, duration, severity, area, intensity, distance, and direction of drought trajectory) are used to quantify drought events from the 3D perspective leading to contribute to the creation of

Fig. 1. Outlines of the study area bounded by a latitude of 50°N.

Table 1
Drought severity classified by the SPEI.

Classes	SPEI	Severity
1	$-1.0 < \text{SPEI}$	No drought
2	$-1.5 < \text{SPEI} \leq -1.0$	Moderate drought
3	$-2.0 < \text{SPEI} \leq -1.5$	Severe drought
4	$\text{SPEI} \leq -2.0$	Extreme drought

dynamic drought maps. Finally, based on dynamic drought maps, we present a novel drought monitoring approach that can quantify the evolutionary characteristics of developing drought events on both temporal and spatial scales.

2. Data and methods

2.1. Study area

The study area, as shown in Fig. 1, consists of six countries: Tajikistan, Kazakhstan, Turkmenistan, Uzbekistan, part of China, and Kyrgyzstan. As the precipitation data used in this study is only available for regions below 50°N, the study area had to be cropped accordingly. The countries within Central Asia have high climatic contrasts. Generally, across the region, winters are moderate to cool, with mean temperatures ranging from − 3–20 °C, while summers are warm to hot, with mean temperatures ranging from 20 °C to 40 °C. Winter temperatures can drop as low as − 45 °C and go as high as 50 °C in summer (Broka et al., 2016). Precipitation also varies across the region where the average annual precipitation is 500 mm in Tajikistan and 250 mm in Uzbekistan (USAID, 2018). In Central Asia, 80% of the land surface has a higher sensitivity to precipitation anomalies, while temperature is becoming an important parameter in drought assessment to account for the potential impact of climate change on arid regions. That is, even if there is no significant change of precipitation, an increase of the atmospheric temperature will increase the rate of evaporation and evapotranspiration, which may reduce available water resources in Central Asia (Mirzabaev, 2013). For the drought analysis of the Central Asia region, it is appropriate to use the drought index based on precipitation and temperature, which considers the effect of evapotranspiration on drought.

2.2. Standardized precipitation evapotranspiration index (SPEI)

SPEI is a multi-scale drought index based on a water balance and is widely used to assess drought conditions. This index reflects the extent to which a region deviates from the average drought year, with negative values representing more evaporation than precipitation and positive values representing more precipitation than evaporation.

To estimate the SPEI value, the difference of the water balance was normalized to a log-logistic probability distribution (Vicente-Serrano et al., 2010), of which the probability density function and cumulative distribution function are given in Eqs. (1) and (2), respectively.

$$f(x) = \frac{\beta}{\alpha}\left(\frac{x-\gamma}{\alpha}\right)\left[1+\left(\frac{x-\gamma}{\alpha}\right)\right]^{-2} \tag{1}$$

$$F(x) = \left[1+\left(\frac{\alpha}{x-\gamma}\right)^{\beta}\right]^{-1} \tag{2}$$

where α, β, and γ are parameters representing the scale, shape, and location, respectively.

Vicente-Serrano (2006) calculated the SPEI as follows:

$$SPEI = W - \frac{C_0 + C_1 W + C_2 W^2}{1 + d_1 W + d_2 W^2 + d_3 W^3} \tag{3}$$

where $C_0 = 2.5155$, $C_1 = 0.8028$, $C_2 = 0.0203$, $d_1 = 1.4327$, $d_2 = 0.1892$, and $d_3 = 0.0013$. When $P \leq 0.5$, $W = \sqrt{-2\ln(P)}$ and when $P > 0.5$, $W = \sqrt{-2\ln(1-P)}$.

The drought severity is classified by the SPEI, as shown in Table 1.

Pyarali et al. (2022) presented a high-resolution (5 km) standardized precipitation evaporation index (SPEI-HR) for Central Asia at various time scales from 1981 to 2018 using Climate Hazards group InfraRed Precipitation with Station's (CHIRPS) precipitation and Global Land Evaporation Amsterdam Model's (GLEAM) potential evaporation (Ep) datasets. The available observed meteorological data of the region is not continuous and very scarce for the entirety of Central Asia. The SPEI-HR dataset was developed to overcome the lack of data for monitoring the effects of drought in Central Asia. In this study, we utilized 6-month time scale of SPEI-HR data covering the period from 1981 to 2018 for the characteristics analysis of 3D-drought events.

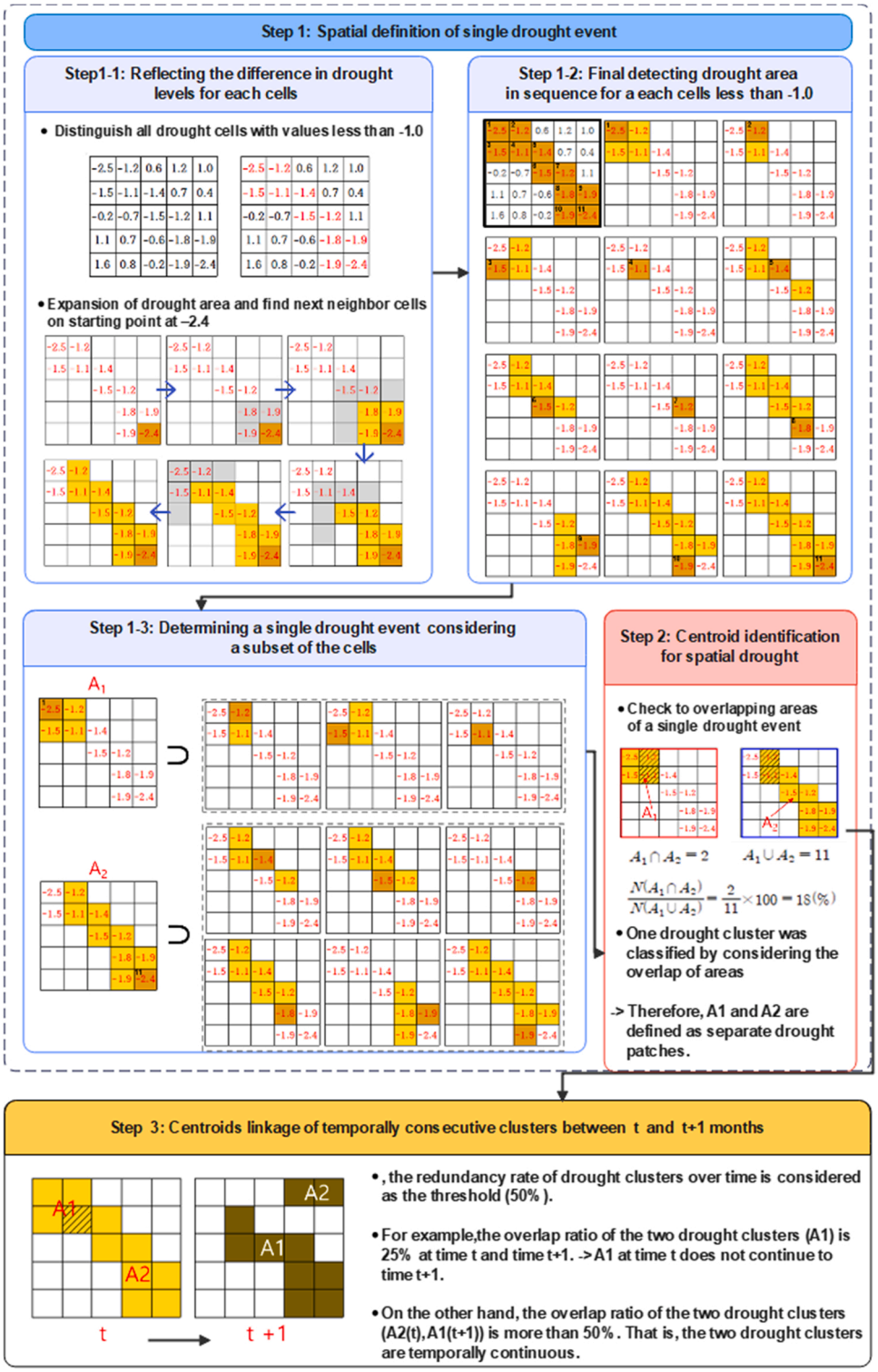

Fig. 2. Procedure of the dynamic drought detection technique (DDDT) algorithm.

2.3. Dynamic drought detection technique (DDDT) algorithm

In general, to identify drought events in a 3D concept, a continuous grid is divided into clusters (2D spatial clusters) on a spatial scale and then defined as a 3D-drought event by examining connectivity on a time scale (Rulinda et al., 2013). In this study, in

screening 3D drought events, the assumption that it occurs when adjacent grids are in a drought state in both temporal and spatial dimensions is still followed (Guo et al., 2018). However, the DDDT algorithm proposed in this study is different from previous studies in the process of clustering the grid on the spatial scale and the method of determining the center of drought. In this study, the dynamic evolution of drought was analyzed using the DDDT algorithm as follows.

Step 1: Spatial definition of a single drought event.

At the spatial scale, a drought cluster is identified by continuous drought area (CDA) analysis (Corzo Perez et al., 2011; Lloyd-Hughes, 2012; Van Huijgevoort et al., 2013; Herrera-Estrada et al., 2017; Diaz et al., 2020). The CDA analysis follows a connected component labeling approach for clustering drought cells (Haralick and Shapiro, 1992) by applying a two-scan algorithm. First, each cell is numbered for a location. The binary grid is then navigated to perform the first run, which assigns temporary labels to connected (adjacent) components (cells). This label represents the connection between the eight closest neighbors and all cells. A 3×3 cell section was used in this study, with a total of nine cells in the grid and eight perimeters in the centroid cell. More detail information on the CDA analysis is provided in Corzo Perez et al. (2011).

However, when clustering drought regions based on the CDA, only the presence of drought classified by a specific threshold is adapted without considering the grid-based severity of drought. That is, clustering droughts on a spatial scale based on grid-specific binary (0 and 1) values, we assume the grid-by-grid drought intensity is uniform. Therefore, in this study, a new concept of clustering spatial drought areas was proposed by considering the difference of drought severities by grid. This means that the spatial drought extent is centered on the grid with the greatest severity at a specific time, and the drought intensity is propagated to the adjacent grid. Therefore, the grid can be clustered by considering the size of the drought severity of the original grid rather than the binary value (0, 1).

Step 2: Centroid identification for spatial drought.

In previous studies, researchers identified a major drought cluster (e.g., the cluster with the largest drought area) at a specific time and defined the centroid (p) of the cluster as the centroid at each time step (Corzo Perez et al., 2011; Lloyd-Hughes, 2012). That is, at each time step, only one center of the drought cluster is determined. However, when determining the center of drought according to this method, the case with a large drought severity in a cluster with a small area may be overlooked. In addition, mild droughts that occur over large areas may be overestimated, leading to the selection of drought centers (Diaz et al., 2020). Therefore, in this study, we did not intend to decide on one clustering on the spatial scale every time. The overlapping area ratio of spatially adjacent clusters was reviewed using Eq. (4) for all the 2D drought clusters classified in step 1 as a target. When the overlapping area ratio was 75% or more, they were reclassified into one cluster and the centroid's equation is detailed in Wang et al. (2019).

For example, as shown in Eq. (4), A_1 and A_2 were merged by the threshold (i.e., spatial overlap ratio) into one cluster, where the overlap ratio of areas between single drought events (A_1 and $_{A2}$) was 75% or more. The cell with the lowest SPEI was selected as the centroid of drought in each cluster.

$$Spatial \quad overlap \quad ratio \quad (\%) = \frac{Area(A_1 \cap A_2)}{Area(A_1 \cup A_2)} \times 100 \quad (\%) \tag{4}$$

Step 3: Centroid linkage of temporally consecutive clusters.

A rule that separates or joins time sequences is required to link the centroids of a continuous cluster over time. In this study, the redundancy rate of the drought clusters over time was considered as the threshold (i.e., temporal overlap ratio). The two clusters were defined as having temporal continuity when the ratio of the overlapping area to the area of a relatively large community between the area of the community at time t (A_t) and at time $t + 1$ (A_{t+1}) was 50% or more, as shown in Eq. (5). The rules for connecting the centroids of the clusters are shown in Fig. 2.

$$Temporal \quad overlap \quad ratio \quad (\%) = \frac{A_{overlap}(t, t+1)}{\max(A_t, A_{t+1})} \times 100(\%) \tag{5}$$

2.4. Spatiotemporal characteristics of droughts

The spatiotemporal characteristics of a drought can be explained using indicators such as drought duration, severity, affected area, intensity, location of drought centroid (latitude and longitude), and the distance and direction of the drought trajectory.

1) Drought duration is determined by the period between the beginning and the end of the drought in space and time, meaning the time at which the drought centroids are connected.
2) Drought severity is the sum of the cumulative severities of the affected grid during the drought duration. The drought threshold (SPEI < -1.0) was used to determine a 3D-drought event, as in Table 1.
3) Drought area is defined as the number of the affected grids during the drought duration. The area per grid is 25 km^2 in this study.
4) Drought intensity is the severity divided by the duration of drought.
5) Drought centroid is the cluster's centroid at the spatial scale. It is calculated by weighted average considering the drought severity for each grid.
6) Distance of the drought trajectory is calculated as the sum of distance between centroids for a 3D-drought event.
7) Direction of the drought trajectory is determined based on the location where the 3D-drought event started (latitude, longitude) and the location where it ended (latitude, longitude).

Table 2
Rules and directions for the initial and end points of the track.

Id	Rule	Direction	Id	Rule	Direction
1	$0 \leq \theta < 11.25$ or $348.75 \leq \theta < 360$	E	9	$168.75 \leq \theta < 191.25$	W
2	$11.25 \leq \theta < 33.75$	ENE	10	$191.25 \leq \theta < 213.75$	WSW
3	$33.75 \leq \theta < 56.25$	NE	11	$213.75 \leq \theta < 236.25$	SW
4	$56.25 \leq \theta < 78.75$	NNE	12	$236.25 \leq \theta < 258.75$	SSW
5	$78.75 \leq \theta < 101.25$	N	13	$258.75 \leq \theta < 281.25$	S
6	$101.25 \leq \theta < 123.75$	NNW	14	$281.25 \leq \theta < 303.75$	SSE
7	$123.75 \leq \theta < 146.25$	NW	15	$303.75 \leq \theta < 326.25$	SE
8	$146.25 \leq \theta < 168.75$	WNW	16	$326.25 \leq \theta < 348.75$	ESE

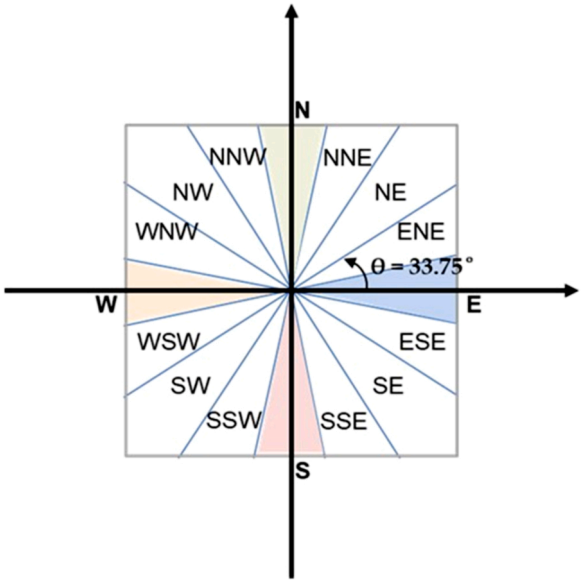

Fig. 3. Schematic diagram for the migration direction of a drought.

Table 3
Descriptive statistics for drought events based on the DDDT algorithm.

Total number of drought events: 32,274					
	Drought duration (months)	Drought severity (-)	Drought area (km^2)	Drought intensity (-)	Trajectory distance (km)
Min	2.00	12.30	300.00	6.15	0.00
Mean	3.65	553.57	9562.27	127.22	37.80
Max	32.00	14,859.36	230,900.00	1895.75	746.25
Standard Deviation	2.39	820.58	13,118.21	120.31	49.96

Table 2 describes how to distinguish the direction of drought trajectory. Fig. 3 presents the schematic diagram for identifying the migration direction of a drought, where the angle θ is in the range of 0–360°. The direction of the migration path is interpreted as follows: the positive eastern direction from the origin of the coordinate system with respect to the first drought centroid (initial centroid) is represented on the horizontal axis. Furthermore, θ between the horizontal axis and the line connecting the origin and the centroid of the last drought (the last centroid) represents a value for determining the migration direction. As shown in Table 2, the centroid of a particular cluster is located in one of 16 proposed positions.

3. Results and discussion

3.1. 3D-drought event analysis based on the DDDT algorithm

The DDDT algorithm was applied to define spatiotemporal drought events in Central Asia. These droughts are considered as a continuum in three dimensions (longitude, latitude, time), i.e., drought patches clustered in the 2D space must be continuously

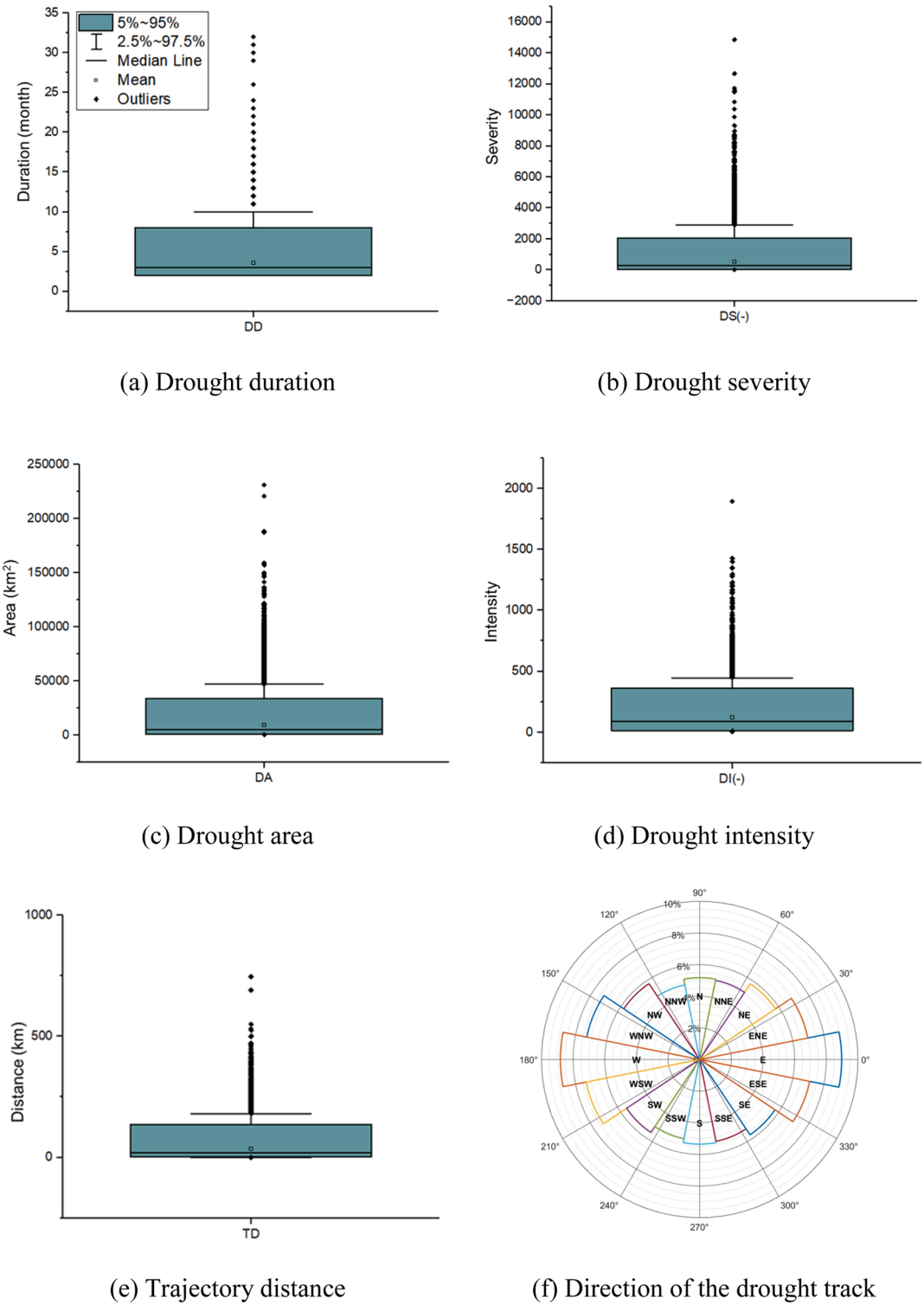

Fig. 4. Statistical characteristic for 3D-drought properties in Central Asia.

connected in the temporal dimension to be grouped into one final cluster (3D-drought event). Table 3 and Fig. 4 show the results of extracting 3D-drought events in Central Asia by applying this method. During the period of 1981–2018, according to the estimated SPEI6-HR, a total of 32,274 drought events lasting more than two months occurred.

In this study, the characteristics of the occurrence of drought in Central Asia were summarized using six indices that characterize

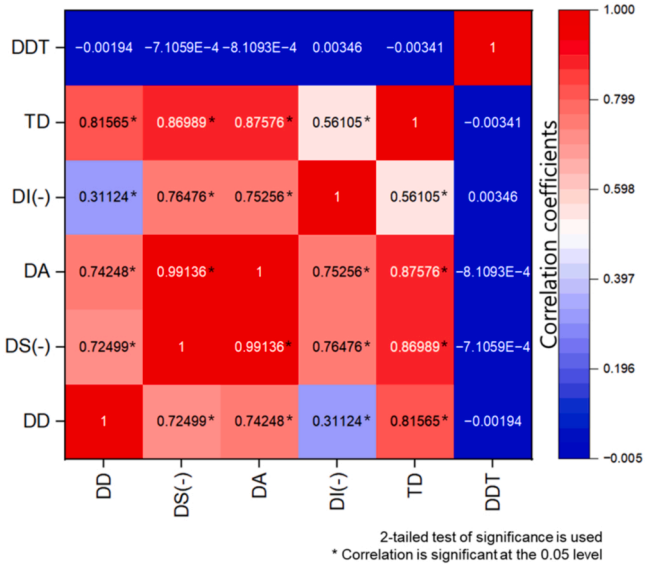

Fig. 5. The Pearson correlation coefficients heat map between 3D-drought properties.

the spatiotemporal evolution of drought phenomena. The distributions of the values for each indicator are shown in Fig. 4. Fig. 4(a)-(e) show box-plots of each indicator for the 3D-drought events, showing the characteristics of the movement direction of the drought trajectory based on the location information of the center. It was found that most of the trajectories of droughts occurring in Central Asia moved in the lateral direction, east and west (ENE, E, ESE, WNW, W, WSW).

Pearson correlation analysis was performed to analyze the statistical characteristics of spatiotemporal evolution using the 3D-drought event characteristic indicator. The Pearson correlation coefficients between drought duration (DD), drought severity (DS), drought area (DA), drought intensity (DI), trajectory travel distance (TD), and drought trajectory travel direction (DDT) are shown in Fig. 5.

It was confirmed that the drought duration, severity, area, and trajectory movement distance indicators had a high correlation (0.7–0.9) with each other. On the other hand, for drought intensity, the correlations between drought duration ($r = 0.31$) and travel distance ($r = 0.56$) were low. However, the direction of movement of the drought trajectory had no correlation with the drought duration, severity, area, intensity, or distance traveled.

Table 4 presents the top 20 most severe drought events in Central Asia from 1981 to 2018. The most severe drought event was based on the drought severity (sum of SPEIs (values below –1) affected by the grid during the drought duration) that had the highest correlation with other indicators among the six drought indicators reviewed above. Table 4 shows the characteristics (beginning(B) time, end(E) time, duration, severity, area, intensity, movement distance, and trajectory direction) of the most severe drought events (top 20) in Central Asia.

The most severe drought occurred in Kyrgyzstan, which started in October 2007 and continued for 11 months. This drought showed a lateral movement trajectory to the west ($\theta = 180.71$) and the affected area during the duration of the drought was 230,900 km^2, which is larger than the area of Kyrgyzstan (199,900 km^2). The second most severe drought occurred in Uzbekistan. Beginning in August 1985, the drought continued for 12 months. This drought showed a movement trajectory in the north-northeast ($\theta = 61.25$) direction and the affected area during the drought was 220,850 km^2.

Based on the drought occurrence times indicated by the bolds in Table 4, the drought events that occurred within the period of 2007–2008 accounted for 35% (7 out of 20) of the total number of droughts. In fact, during 2007–2008, there were severe droughts in Turkmenistan, Tajikistan, and Kyrgyzstan (Food and Agriculture Organization FAO, 2017). Accordingly, it is effective to use the 3D-drought event identification technique based on the DDDT algorithm in characterizing and understanding the spatiotemporal evolution of drought phenomena.

3.2. A new drought monitoring approach using conditional filtering

The DDDT algorithm proposed in this study has an advantage in explaining the developmental process and evolutionary characteristics of drought phenomena. This method determines 3D- drought events to quantify the continuous and dynamic evolutionary (developmental) characteristics of drought events in the 3D space. In particular, this method can identify all drought events in the long-term drought time series.

In previous studies, when a drought event was identified using the 3D clustering method, the occurrence of drought in the grid was distinguished according to the binary number system in determining the spatial drought patch, which is a 2D concept (Xu et al., 2015; Guo et al., 2018). On the other hand, the DDDT algorithm proposed in this study clusters the spatial drought patch by considering that

Table 4
Characteristics of the top 20 3D-drought events based on the DDDT algorithm using SPEI-HR in Central Asia.

Top 20	Beginning time	End time	DD (months)	DS (-)	DA (km^2)	DI (-)	TD (km)	DDT (θ)	Lon. (B) (°E)	Lat. (B) (°N)	Lon. (E) (°E)	Lat. (E) (°N)
1	**2007/10**	**2008/08**	11	**14,859.36**	230,900	1350.85	472.45	180.71	71.20	41.61	69.24	41.58
2	1985/08	1986/07	12	**12,671.32**	220,850	1055.94	468.24	61.25	68.95	42.20	69.53	43.26
3	1983/12	1985/02	15	**11,728.22**	157,125	781.88	365.22	257.41	57.91	47.42	57.79	46.88
4	1983/04	1985/02	**23**	**11,573.22**	188,400	503.18	501.78	72.14	56.29	46.06	56.76	47.53
5	1993/12	1996/04	**29**	**11,491.32**	187,525	396.25	690.63	261.17	74.61	49.84	74.40	48.46
6	1983/04	1984/10	19	**10,845.64**	146,325	570.82	498.46	91.21	58.86	46.36	58.82	48.47
7	1982/12	1983/07	8	**10,384.72**	158,425	1298.09	361.56	316.21	70.82	45.54	71.93	44.47
8	1994/09	1995/08	12	**9866.73**	158,950	822.23	366.12	66.63	70.62	45.72	71.29	47.26
9	**2007/11**	**2009/01**	15	**9332.58**	136,625	622.17	314.82	251.89	84.94	48.19	84.63	47.22
10	**2007/09**	**2008/10**	14	**9313.05**	149,675	665.22	437.35	64.43	70.67	40.64	71.30	41.97
11	**2007/12**	**2008/12**	13	**8959.96**	127,850	689.23	336.07	168.18	82.80	46.54	82.53	46.60
12	1994/09	0996/03	19	**8730.54**	147,375	459.50	437.00	80.71	74.62	42.08	74.86	43.56
13	1983/12	1995/01	14	**8674.49**	111,250	619.61	322.60	38.46	58.08	45.96	58.40	46.22
14	**2007/10**	**2008/09**	12	**8671.28**	141,325	722.61	411.52	140.03	71.30	41.79	70.08	42.82
15	1997/04	1998/01	10	**8624.31**	110,150	862.43	394.63	163.07	85.70	47.11	83.63	47.74
16	**2007/09**	**2008/11**	15	**8576.75**	135,675	571.78	345.51	147.65	73.72	41.34	72.77	41.94
17	1991/05	1992/02	10	**8464.35**	130,250	846.44	412.96	346.89	70.62	48.34	71.03	48.24
18	**2008/01**	**2008/12**	12	**8446.74**	133,925	703.90	293.11	20.79	86.57	48.06	87.26	48.32
19	**1994/09**	**1996/06**	**22**	**8446.16**	134,100	383.92	531.84	6.83	73.42	48.61	74.72	48.76
20	1991/04	1991/12	9	**8443.59**	132,725	938.18	310.89	216.13	73.98	47.64	72.97	46.90

the grid with a large drought depth becomes the center and transfers (spreads) to adjacent grids in determining the occurrence of drought in the grid. Accordingly, it is possible to quantify the dynamic development characteristics of drought events by sufficiently considering the scale of drought depth for each grid.

A drought event identified in this way can be shown in Fig. 6 as a dynamic drought map that includes all the drought attributes in the 3D aspect. Fig. 6(a) is a diagram comparing a typical drought map with a dynamic drought map. The typical drought map on the left panel shows the drought index values for a specific month using SPEI6-HR data. In contrast, the dynamic drought map on the right panel contains drought characteristics for drought events identified through the DDDT algorithm. Therefore, in the dynamic drought map, clustered drought patches are characteristic in consideration of the continuity and dynamics of drought events. Fig. 6(b) shows a conceptual diagram of the characteristic variables of 3D drought events (dry start time, drought center, drought affected area, center movement trajectory, and movement direction).

In this study, we intended to explore various methods that can utilize dynamic drought maps including 3D drought attributes. For example, a conditional drought monitoring approach is helpful to determine whether a drought patch included in a dynamic drought map is new at this time or whether a drought patch that occurred in the past has continued to the present time.

The upper graphs in Fig. 7 are time series plots of the number of drought patches per month during the drought period in Central Asia. As shown in Fig. 6(b), the dynamic drought map contains information that can confirm the continuity and dynamics of past drought events for each patch. That is, except for the drought patch in which the temporal continuity of the drought event exists, the remainder is classified as a newly appeared drought patch in the current month.

The bottom graphs of Fig. 7 show the drought monitoring information divided through the new conditional drought monitoring approach. The orange bars represent the case of drought duration is one month, classified as a drought patch newly generated every month. On the other hand, the green bars represent the case of drought duration is more than 2 months, in which the drought events that have occurred in the past have continuity until the current month. It was confirmed that when the number of drought patches rapidly increases (2002/02–03, 2007/09–10), the proportion of drought patches newly generated in the current month increases

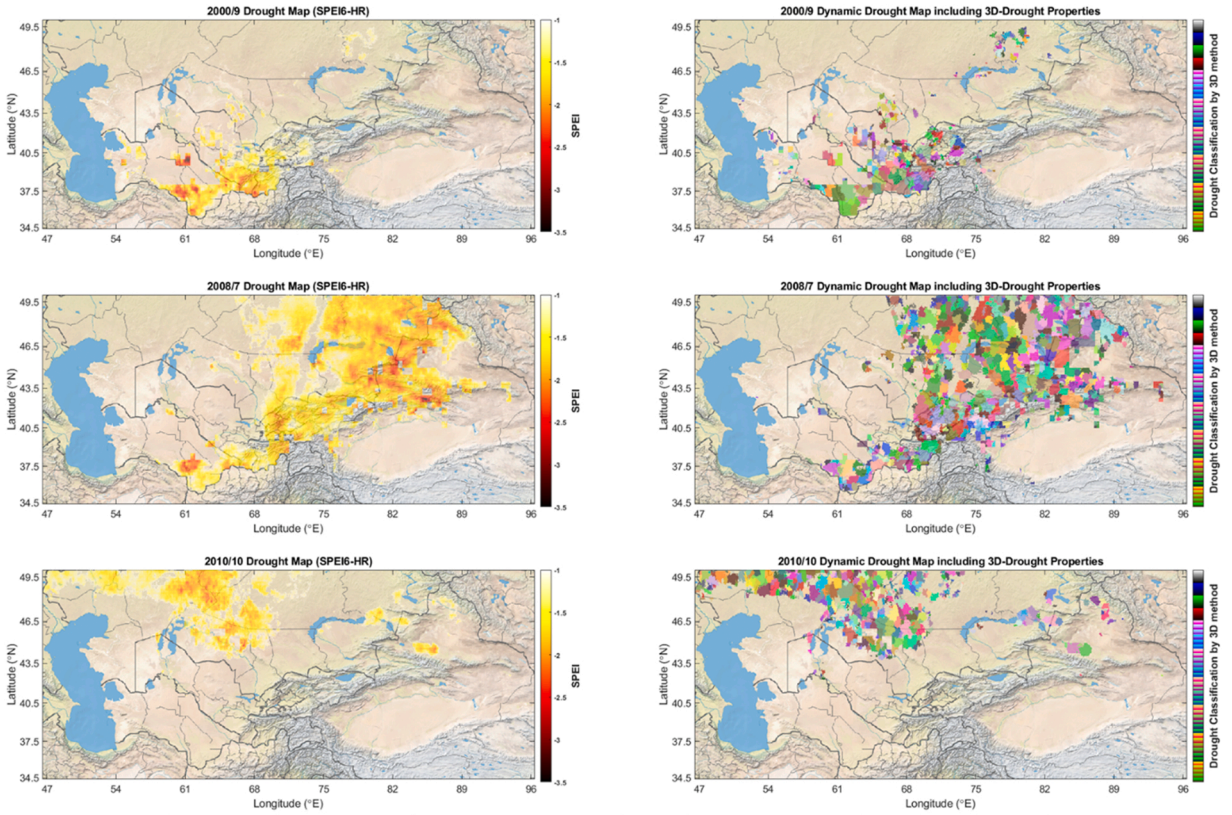

(a) Drought map (SPEI6-HR) and dynamic drought map including 3D-drought properties

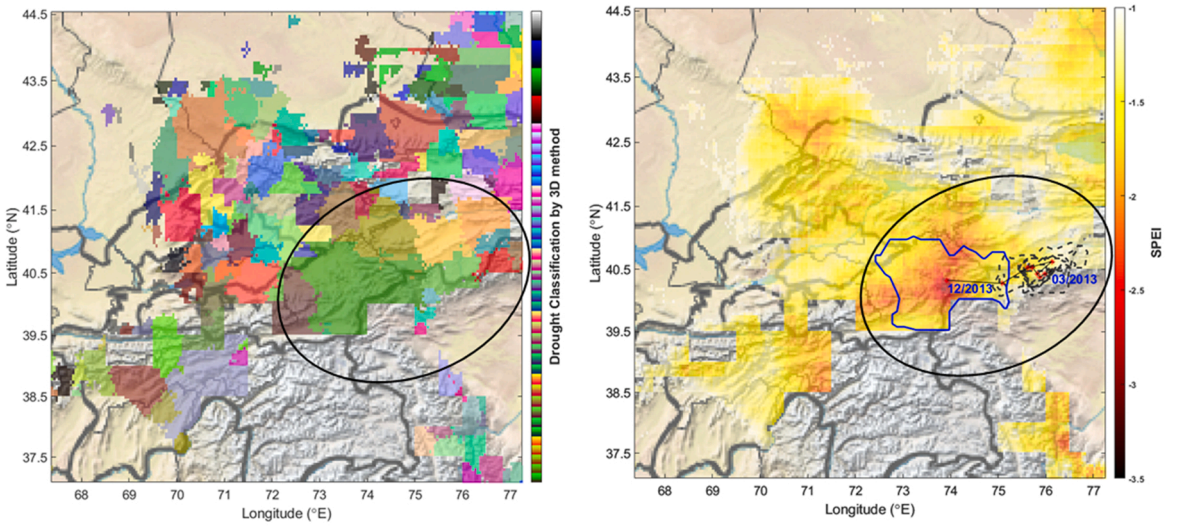

(b) Drought trajectories and extent of impact for patches separated by 3D-drought events

Fig. 6. Conceptual explanation for 3D-drought properties in a dynamic drought map.

significantly. In contrast, when the number of drought patches continues to increase steadily over a long period of time (2010/6–2011/1), the proportion of past drought patches increases significantly. In addition, the number of drought patches decreased sharply from February to July 2011, but it was confirmed that drought patches that occurred in the past persisted for a long time. To verify the effectiveness of the conditional drought monitoring technique based on the dynamic drought map, it is necessary to compare and review the actual recorded drought cases with the results obtained through drought monitoring.

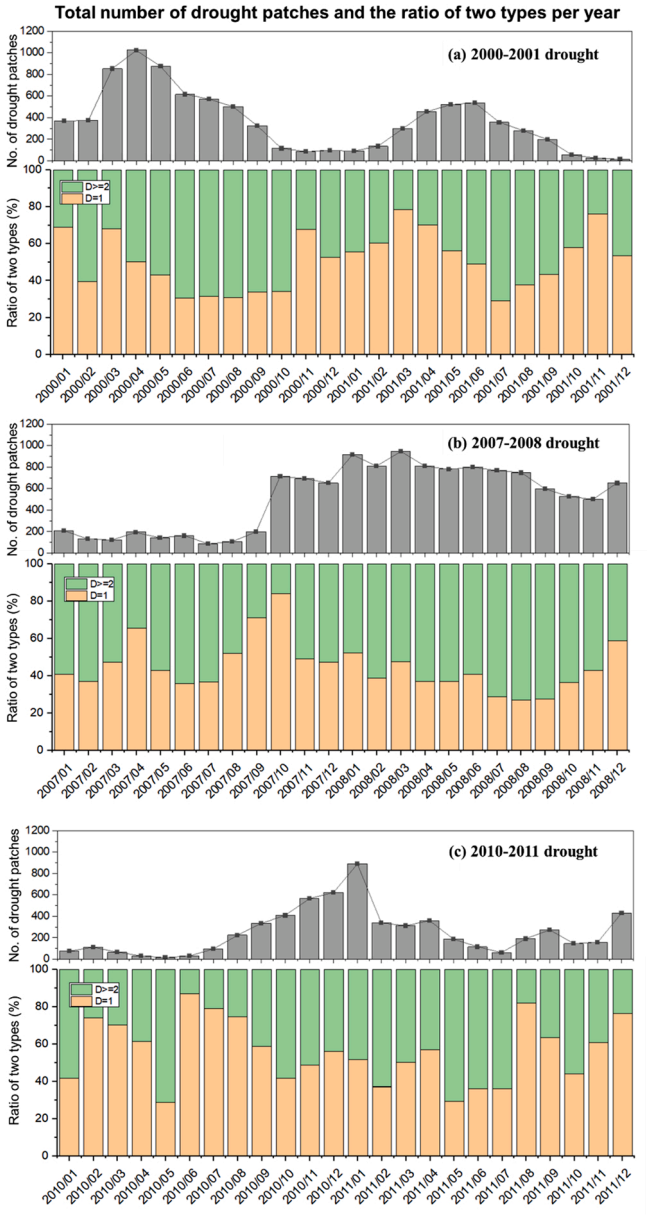

Fig. 7. Results of applying a new conditional drought monitoring approach in Central Asia.

Fig. 8 shows the results of dividing the data into two types of monthly drought patches identified in Central Asia from 1981 to 2018, where the y-axis represents the number of monthly drought patches. Here, type #1 is the number of new drought patches that occurred in the current month and type #2 is the number of drought patches that occurred from the time before the corresponding month and continued until the current month. Comparing the number of drought patches of the two types per month, it was confirmed that there was a delay time between the time series of type #1 and type #2, when a newly created drought patch continued into the next month. In addition, depending on the characteristics of the occurrence of new drought patches up to a specific month, it causes a change in the number of drought patches of type #2.

For example, after January 1983, when the type #1 drought patch rapidly increases with a steep slope, most of it leads to type #2, except for the case of a flash drought of less than one month. However, when the type #1 drought patch steadily increases over a long period of time, such as after June 1993, the type #2 drought patch has a large cumulative effect due to the type #1 drought patch. In December 2007, the number of type #1 drought patches appeared to gradually decrease. However, at this time, the number of type #2 drought patches continued to increase and then changed to a decreasing trend after 9 months. Accordingly, when forecasting future droughts based on data built through dynamic drought monitoring, it will be useful information to understand the spatiotemporal patterns of the droughts that have occurred in the past.

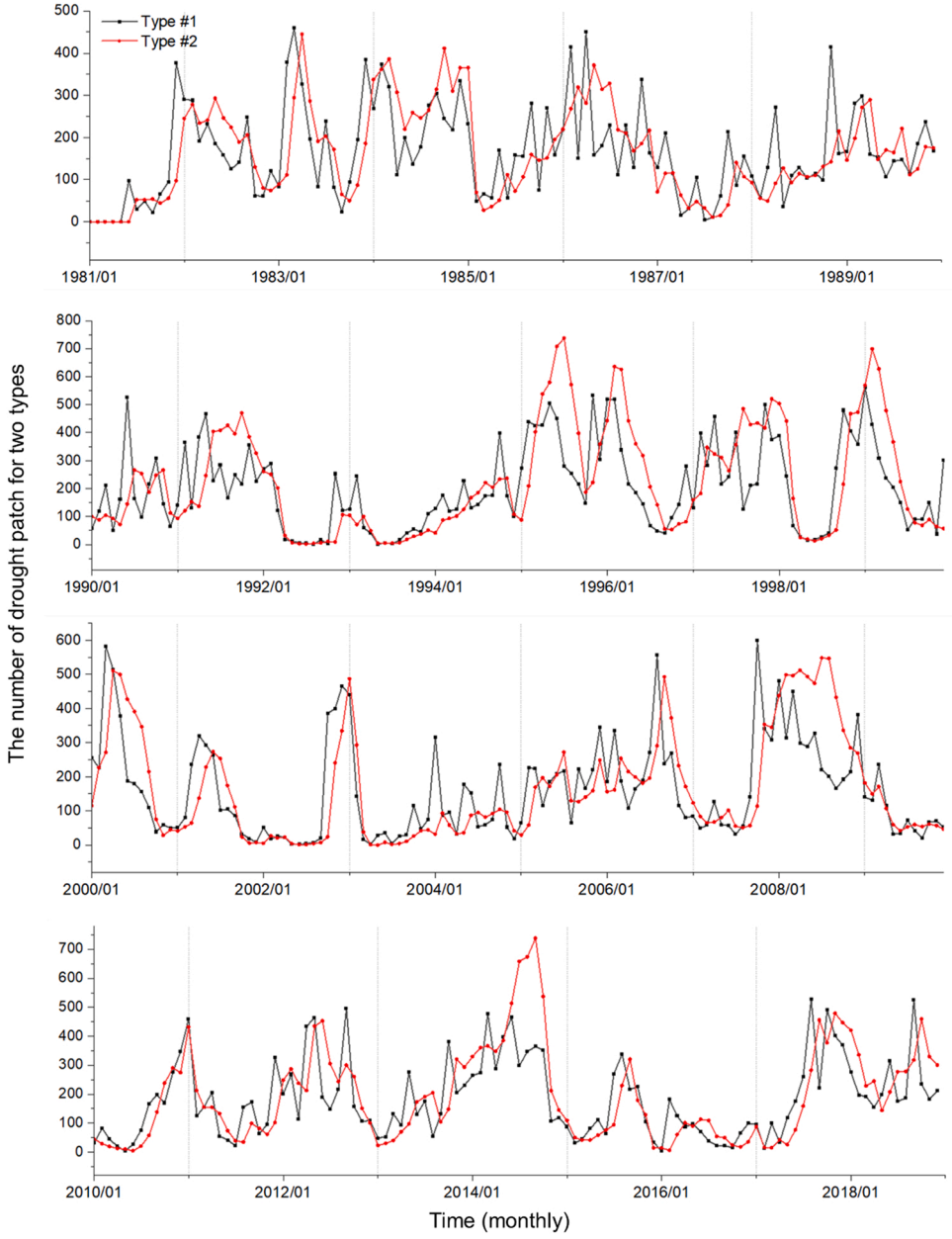

Fig. 8. Classification of two types of drought patches through conditional filtering based on a new drought monitoring approach.

4. Conclusions

In this study, we proposed a dynamic drought monitoring method based on a 3D drought event selected by applying the dynamic drought monitoring technique algorithm. In addition, considering the climate (typical temperate continental climate) of Central Asia and various topographical characteristics (mountainous terrain, low-lying basin, desert, and grassland), the most suitable data for drought monitoring (high resolution (5 km) SPEI-HR drought dataset) was carefully selected and utilized. In addition, the spatial and temporal distribution characteristics of drought events and the movement characteristics of dynamic drought trajectories were analyzed by a 3D concept utilizing the DDDT algorithm for droughts in Central Asia.

The dynamic drought characteristics are explained through a 3D clustering method based on the DDDT algorithm, which were defined as 3D-drought events, which included various drought characteristic indicators (drought durations, severity, effected area, intensity, location (latitude and longitude), distance and direction of the drought trajectory) to quantify the spatiotemporal evolutionary characteristics of drought events. Then, we proposed a new conditional drought monitoring approach that can explain the developmental process and evolutionary characteristics of drought phenomena using a 3D concept. In this study, several conclusions

were drawn as follows.

(1) In characterizing the evolution of spatial drought, the DDDT algorithm does not cluster according to the occurrence of drought (1 or 0). In other words, the actual size of the drought depth for each grid is fully reflected and clustered. It also follows the basic assumption that the drought magnitude of the adjacent grid around the grid with the maximum drought depth is mitigated. It is based on the concept that the effects of a drought spread to neighboring regions, centered on the maximum depth of drought. This is a useful concept for consistency in determining one centroid per drought patch.
(2) In the past, the evolution of spatiotemporal drought was characterized by focusing on the largest drought event. However, if the DDDT algorithm is applied using a high-resolution drought data set, it is possible to identify all mild drought events that have been easily overlooked.
(3) During the period of 1981–2018, the drought trajectories in Central Asia tended to move horizontally to the east and west. Central Asia droughts have very strong correlations among the duration, depth, area, and travel distance indicators of trajectories. This has the advantage of being clear in determining one criterion (indicator) among various indicators in determining the most severe drought event.
(4) The dynamic drought map including all 3D-drought properties would be useful for conditional drought monitoring. In other words, when using the dynamic drought map, even information that cannot be confirmed in a general drought map, such as the temporal continuity and dynamic evolution characteristics of drought events, can be intuitively identified.

In this study, only one filtering condition (two types of patch classification: type #1 and type #2) was used to apply the conditional drought monitoring approach. However, there will be countless other drought information that can be obtained by using dynamic drought maps. Therefore, in a follow-up study, we intend to develop various filtering contents necessary to increase the utilization of the new conditional drought monitoring approach proposed in this study. This will help to discover the characteristics of spatiotemporal drought patterns in the Central Asia region. Furthermore, it will be valuable as numerical data that can be used for short-term and long-term drought forecast studies.

Funding

This work was supported by the National Research Foundation of Korea funded by the Korean government (No. NRF-2020R1C1C1014636) and the Korea Environment Industry & Technology Institute (KEITI) through Water Management Innovation Program for Drought (No. 2022003610001) funded by Korea Ministry of Environment.

CRediT authorship contribution statement

Jiyoung Yoo: Conceptualization, Methodology, Writing – original draft. **Jiyoung Kim**: Data curation, Visualization. **Hyun-Han Kwon**: Investigation, Validation. **Tae-Woong Kim**: Supervision, Writing – review & editing.

Declaration of Competing Interest

The authors declare that they have no known competing financial interests or personal relationships that could have appeared to influence the work reported in this paper.

Data availability

Data will be made available on request.

References

Andreadis, K.M., Clark, E.A., Wood, A.W., Hamlet, A.F., Lettenmaier, D.P., 2005. Twentieth-century drought in the conterminous United States. J. Hydrometeorol. 6, 985–1001. https://doi.org/10.1175/JHM450.1.

Broka, S., Giertz, Å., Christensen, G., Rasmussen, D., Morgounov, A., Fileccia, T., Rubaiza, R., 2016. Kazakhstan agricultural sector risk assessment. Agriculture Global Practice Technical Assistance Paper. World Bank. License: CC BY 3.0 IGO. ⟨https://open-knowledge.worldbank.org/handle/10986/23763⟩.

Cook, E.R., Meko, D.M., Stahle, D.W., Cleaveland, M.K., 1999. Drought reconstructions for the continental United States. J. Clim. 12, 1145–1162. https://doi.org/10.1175/1520-0442(1999)012%3C1145:DRFTCU%3E2.0.CO;2.

Corzo Perez, G.A., van Huijgevoort, M.H.J., Voß, F., van Lanen, H.A.J., 2011. On the spatio-temporal analysis of hydrological droughts from global hydrological models. Hydrol. Earth Syst. Sci. 15, 2963–2978. https://doi.org/10.5194/hess-15-2963-2011.

Diaz, V., Corzo Perez, G.A., Van Lanen, H.A.J., Solomatine, D., Varouchakis, E.A., 2020. An approach to characterise spatio-temporal drought dynamics. Adv. Water Resour. 137, 103512 https://doi.org/10.1016/j.advwatres.2020.103512.

Food and Agriculture Organization (FAO), 2017. Drought characteristics and management in Central Asia and Turkey. FAO Water Rep. 114.

Gocic, M., Trajkovic, S., 2014. Spatiotemporal characteristics of drought in Serbia. J. Hydrol. 510, 110–123. https://doi.org/10.1016/j.jhydrol.2013.12.030.

Guo, H., Bao, A., Ndayisaba, F., Liu, T., Jiapaer, G., El-Tantawi, A.M., De Maeyer, P., 2018. Space-time characterization of drought events and their impacts on vegetation in Central Asia. J. Hydrol. 564, 1165–1178. https://doi.org/10.1016/j.jhydrol.2018.07.081.

Haralick, R.M., Shapiro, L.G., 1992. Computer and Robot Vision, vol. 1. Addison-Wesley Longman Publishing Co., Inc., Boston, U.S.A.

Herrera-Estrada, J.E., Satoh, Y., Sheffield, J., 2017. Spatio-temporal dynamics of global drought. Geophys. Res. Lett. 44, 2254–2263. https://doi.org/10.1002/2016GL071768.

Hisdal, H., Tallaksen, L.M., 2003. Estimation of regional meteorological and hydrological drought characteristics: a case study for Denmark. J. Hydrol. 281, 230–247. https://doi.org/10.1016/S0022-1694(03)00233-6.
Liu, X., Pan, Y., Zhu, X., Yang, T., Bai, J., Sun, Z., 2018. Drought evolution and its impact on the crop yield in the North China Plain. J. Hydrol. 564, 984–996. https://doi.org/10.1016/j.jhydrol.2018.07.077.
Lloyd-Hughes, B., 2012. A spatio-temporal structure-based approach to drought characterisation. Int. J. Climatol. 32, 406–418. https://doi.org/10.1002/joc.2280.
Mirzabaev, A., 2013. Climate volatility and change in Central Asia. Econ. Impacts Adapt. (Available online) ⟨http://hss.ulb.unibonn.de/diss_online/elektronisch⟩.
Oladipo, E.O., 1986. Spatial patterns of drought in the interior plains of North America. J. Clim. 6, 495–513. https://doi.org/10.1002/joc.3370060505.
Pyarali, K., Peng, J., Disse, M., Tuo, Y., 2022. Development and application of high resolution SPEI drought dataset for Central Asia. Sci. Data 9, 172. https://doi.org/10.1038/s41597-022-01279-5.
Rulinda, C.M., Stein, A., Turdukulov, U.D., 2013. Visualizing and quantifying the movement of vegetative drought using remote-sensing data and GIS. Int. J. Geogr. Inf. Sci. 27, 1481–1496. https://doi.org/10.1080/13658816.2012.723712.
Sheffield, J., Andreadis, K.M., Wood, E.F., Lettenmaier, D.P., 2009. Global and continental drought in the second half of the twentieth century: severity–area–duration analysis and temporal variability of large-scale events. J. Clim. 22, 1962–1981. https://doi.org/10.1175/2008JCLI2722.1.
United Nations (UN), 2008. Trends in sustainable development 2008–2009, United Nations Division for Sustainable Development.
USAID, 2018. Climate Risk Profile – Central Asia. ⟨https://www.preventionweb.net/publications/view/59222⟩.
Van Huijgevoort, M.H.J., Hazenberg, P., van Lanen, H.A.J., Teuling, A.J., Clark, D.B., Folwell, S., Gosling, S.N., Hanasaki, N., Heinke, J., Koirala, S., Stacke, T., Voss, F., Sheffield, J., Uijlenhoet, R., 2013. Global multimodel analysis of drought in runoff for the second half of the twentieth century. J. Hydrometeorol. 14, 1535–1552. https://doi.org/10.1175/JHM-D-12-0186.1.
Vicente-Serrano, S.M., 2006. Differences in spatial patterns of drought on different time scales: an analysis of the Iberian Peninsula. Water Resour. Manag. 20, 27–60. https://doi.org/10.1007/s11269-006-2974-8.
Vicente-Serrano, S.M., Beguería, S., López-Moreno, J., 2010. A multiscalar drought index sensitive to global warming: the standardized precipitation evapotranspiration index. J. Clim. 23, 1696–1718. https://doi.org/10.1175/2009JCLI2909.1.
Vidal, J.P., Martin, E., Franchistéguy, L., Habets, F., Soubeyroux, J.M., Blanchard, M., Baillon, M., 2010. Multilevel and multiscale drought reanalysis over France with the Safran-Isba-Modcou hydrometeorological suite. Hydrol. Earth Syst. Sci. 14, 459–478. https://doi.org/10.5194/hess-14-459-2010.
Wang, K., Li, Q., Yang, Y., Zeng, M., Li, P., Zhang, J., 2015. Analysis of spatio-temporal evolution of droughts in Luanhe River Basin using different drought indices. Water Sci. Eng. 8, 282–290. https://doi.org/10.1016/j.wse.2015.11.004.
Wang, Q., Liu, Y.Y., Zhang, Y.Z., Tong, L.J., Li, X., Li, J.L., Sun, Z., 2019. Assessment of spatial agglomeration of agricultural drought disaster in China from 1978 to 2016. Sci. Rep. 9, 1–8.
Wen, X., Liu, Z., Lei, X., Lin, R., Fang, G., Tan, Q., Wang, C., Tian, Y., Quan, J., 2018. Future changes in Yuan River ecohydrology: individual and cumulative impacts of climates change and cascade hydropower development on runoff and aquatic habitat quality. Sci. Total Environ. 633, 1403–1417. https://doi.org/10.1016/j.scitotenv.2018.03.309.
Xu, K., Yang, D., Yang, H., Li, Z., Qin, Y., Shen, Y., 2015. Spatio-temporal variation of drought in China during 1961–2012: a climatic perspective. J. Hydrol. 526, 253–264. https://doi.org/10.1016/j.jhydrol.2014.09.047.
Zhai, J., Huang, J., Su, B., Cao, L., Wang, Y., Jiang, T., Fischer, T., 2016. Intensity–area–duration analysis of droughts in China 1960–2013. Clim. Dyn. 48, 151–168. https://doi.org/10.1007/s00382-016-3066-y.
Zhan, W., Guan, K., Sheffield, J., Wood, E.F., 2016. Depiction of drought over sub-Saharan Africa using reanalyses precipitation data sets, 555–10,574 J. Geophys. Res. Atmos. 121 (10). https://doi.org/10.1002/2016JD024858.